Available online at www.sciencedirect.com
SCIENCE DIRECT
Tetrahedron
ELSEVIER
Tetrahedron 62 (2006) 3412–3422

The enolate anions of chlorophylls *a* and *b* as ambident nucleophiles in oxidations with (−)- or (+)-(10-camphorsulfonyl)oxaziridine. Synthesis of 13^2(*S*/*R*)-hydroxychlorophylls *a* and *b*

Paavo H. Hynninen,[a,*] Tuomo S. Leppäkases[a] and Markku Mesilaakso[b]

[a]*Laboratory of Organic Chemistry, Department of Chemistry, PO Box 55 (A.I. Virtasen Aukio 1), FI-00014 University of Helsinki, Finland*
[b]*Finnish Institute for Verification of the Chemical Weapons Convention, PO Box 55 (A.I. Virtasen Aukio 1), FI-00014 University of Helsinki, Finland*

Received 24 October 2005; revised 16 December 2005; accepted 12 January 2006

Available online 17 February 2006

Abstract—The enolate anions of chlorophylls (Chl) are ambident nucleophiles that are of considerable organic chemical interest in relation to the theory of electron delocalization (aromaticity) and charge-transfer in large conjugated π-systems, as well as for their chemical reactivity. Under deaerated conditions, the (−)- and (+)-enantiomers of (10-camphorsulfonyl)oxaziridine (CSOAI) are effective oxidants for the enolate anions of Chl *a* and Chl *b*, when 1,8-diazabicyclo[5.4.0]undec-7-ene (DBU) serves as a base. In this study, the use of these sterically hindered reagents to hydroxylate Chl *a* and Chl *b* is described for the first time. The total yield of 13^2(*S*/*R*)-HO-Chl *a* was 71 and 90% for the oxidations of Chl *a* with (−)-CSOAI and (+)-CSOAI, respectively. Chl *b*, however, behaved clearly differently from Chl *a*. The total yield of 13^2(*S*/*R*)-HO-Chl *b* was 40% in the oxidation with (−)-CSOAI and 60% in the reaction with (+)-CSOAI. A competing side-reaction, which resulted in the 15^2-methyl, 17^3-phytyl ester of Mg-15^1(*S*/*R*)-unstable rhodin, was found to lower the yields of the desired main products. The formation of the side-products was largely avoided and the yield of 13^2(*S*/*R*)-HO-Chl *b* was improved by increasing the volume of hexane and using phosphate buffer in the first step of the work-up. With (−)-CSOAI, a 94% diastereomeric excess (de) was achieved for 13^2(*R*)-HO-Chl *a*, whereas the de for 13^2(*R*)-HO-Chl *b* was 66%. With (+)-CSOAI, the de was 10% for 13^2(*R*)-HO-Chl *a* and 8% for 13^2(*R*)-HO-Chl *b*. The results were interpreted in terms of a nucleophilic reaction mechanism, kinetically controlled by steric hindrance, originating on the one hand in the 17-propionate phytyl ester side-chain, protruding over the isocyclic ring E of the Chl enolate ion, and on the other hand in the bulky camphorsulfonyl unit of CSOAI. Possible reasons for the different results from the Chl *b* oxidations as compared with those of the Chl *a* oxidations are discussed. Comparison of the differences in the NMR δ_C-values between 13^2(*S*)- and 13^2(*R*)-HO-Chl *a* as well as those between 13^2(*S*)- and 13^2(*R*)-HO-Chl *b*, indicated that the change of stereochemical configuration at C-13^2 induces only slight differences in the δ_C-values. Of special interest are the δ_C-values of C-13^2, which are at ca. 91 ppm for the *a*- and *b*-series diastereomers. This carbon is deshielded by ca. 25 ppm relative to the C-13^2 of 13^2(*R*)-Chl *a* (δ_C=65.5). Owing to this, ^{13}C NMR spectroscopy is a good method to distinguish the 13^2-hydroxylated chlorophylls from the intact, naturally occurring chlorophylls.

1. Introduction

Chlorophyll (Chl) *a* (**1**) and Chl *b* (**5**) occur as pivotal photosynthetic pigments in all green plants. Both chlorophylls, together with carotenoids, are needed to form with protein subunits the light-harvesting Chl *a*/*b* complexes (LHC) of the antenna system (AS), which is responsible for capturing light quanta and conveying the excitation energy to the photosynthetic reaction centre (RC).[1,2] Nevertheless, recent X-ray crystallographic studies[3–5] suggest that only Chl *a* [**1**, 13^2(*R*)-Chl *a*] and/or its close derivatives, such as Chl *a*′ [**2**, 13^2(*S*)-Chl *a*] and pheophytin *a* [**9**, 13^2(*R*)-Pheo *a*], also have the redox-function in the RC, where the excitation energy from AS is converted into chemical energy by a charge separation process. Hence, Chl *b*, in contrast, does not appear to participate in the electron-transfer events of the RC. The chemical basis of this prominent functional difference between Chl *a* and Chl *b* in the photosynthetic process has seldom attracted attention and the comparative investigations in vitro on the chemical reactivities of Chl *a* and Chl *b* have also remained extremely rare. There is another peculiarity, which concerns the difference in behaviour of the two Chls in biological degradation. It has been reported[6] that, in the early stages of plant senescence, endogenous Chl *a* is oxidized to 13^2(*S*/*R*)-HO-Chl *a* (**3**/**4**), but there is no report of the formation of

Keywords: Tetrapyrrole; Porphyrin; Chlorophyll; Oxidation; Enolate; Reaction mechanism; NMR.
* Corresponding author. Fax: +358 9 19150466; e-mail: paavo.hynninen@helsinki.fi

0040–4020/$ - see front matter © 2006 Elsevier Ltd. All rights reserved.
doi:10.1016/j.tet.2006.01.043

13^2(*S*/*R*)-HO-Chl *b* (**7**/**8**) under comparable conditions. To achieve a deeper insight into the reactivity differences between Chl *a* and Chl *b*, we have recently compared the reactivities of the Chls in the Willstätter allomerization reaction (for reviews, see Refs. 7–12), that is, oxidation by ground state (triplet) oxygen, $^3O_2$. Unexpectedly, we found that the two Chls behave differently under comparable reaction conditions. While Chl *a* yielded 13^2(*S*/*R*)-HO-Chl *a* as major oxidation products, Chl *b* in contrast produced only traces of 13^2(*S*/*R*)-HO-Chl *b*. Instead, we found an appreciable amount of an entirely new chlorophyll derivative, the 10-CH_3O-13^2(*S*)-HO-Chl *b* (**13**).[11–16] As the Chl enolate anion is the first intermediate that is highly reactive with $^3O_2$ in the allomerization mechanism, these results can be interpreted as reflecting the electronic differences between the enolate anions[17] of the two chlorophylls, formed through 13^2-deprotonation in the isocyclic ring E, carrying the same enolizable β-keto ester system in both cases.

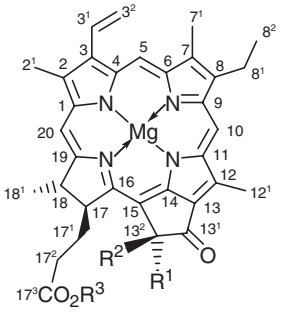

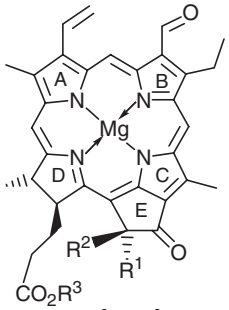

1 R^1=CO_2CH_3; R^2=H; R^3=Phy;
2 R^1=H; R^2=CO_2CH_3; R^3=Phy;
3 R^1=CO_2CH_3; R^2=OH; R^3=Phy;
4 R^1=OH; R^2=CO_2CH_3; R^3=Phy;

5 R^1=CO_2CH_3; R^2=H; R^3=Phy;
6 R^1=H; R^2=CO_2CH_3; R^3=Phy;
7 R^1=CO_2CH_3; R^2=OH; R^3=Phy;
8 R^1=OH; R^2=CO_2CH_3; R^3=Phy;

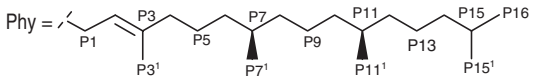

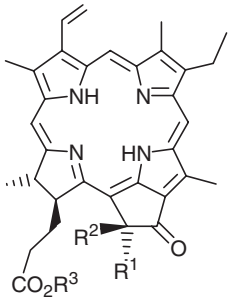

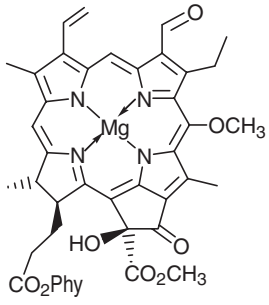

9 R^1=CO_2CH_3; R^2=H; R^3=Phy;
10 R^1=CO_2CH_3; R^2=H; R^3=CH_3;
11 R^1=CO_2CH_3; R^2=OH; R^3=H;
12 R^1=OH; R^2=CO_2CH_3; R^3=H;

13

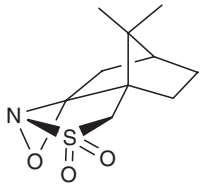

14 (-)-CSOAI

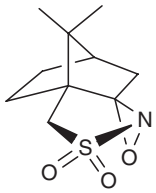

15 (+)-CSOAI

In this investigation, we compare the results from the hydroxylations of the enolate anions of Chl *a* (**1**) and Chl *b* (**5**) using a sterically hindered oxidant, such as the (1*R*)-(−)-enantiomer (**14**) or (1*S*)-(+)-enantiomer (**15**) of (10-camphorsulfonyl)oxaziridine (CSOAI).[18–21] The enolate anion of each Chl is generated with a sterically hindered base, 1,8-diazabicyclo[5.4.0]undec-7-ene (DBU). These reagents were introduced to synthetic organic chemistry by Davies and co-workers[18,19] and were applied by Ma and Dolphin[20,21] to hydroxylate demetallated Chl *a* derivatives, such as pheophytin *a* (**9**) and methyl pheophorbide *a* (**10**). To our knowledge, these reagents have never been applied to hydroxylate Chl *a* and Chl *b* or any of the demetallated Chl *b* derivatives. It is noteworthy that the presence of the central Mg-atom, whose coordination number is 5 or 6, depending on the nature of the nucleophilic solvent, influences the conformation and electronic structure of the whole macrocycle and its peripheral substituents. Therefore, especially with sterically hindered reagents, the outcome of the reaction with an Mg-complexed chlorin would be expected to differ noticeably from that typical of the corresponding metal-free chlorin. This conclusion is supported by the observation that the central Mg-atom makes the Chls more susceptible to allomerization as compared with the corresponding metal-free derivatives.[7,22] In addition, the strongly electron-withdrawing formyl group at C-7 of Chl *b* is expected to have a certain effect on the amounts and species of oxidation products yielded by Chl *b* with CSOAI (**14**/**15**) as compared with those produced by Chl *a*.

Consequently, in our study, we seek to clarify the reactivity differences of Chl *a* and Chl *b* under comparable reaction conditions, both regarding the yields of the major/minor oxidation products as well as regarding the diastereoselectivity of each hydroxylation reaction, expressed in terms of diastereomeric excess (de). We will also examine, with unprecedented thoroughness, a likely mechanism for the reactions. This is done because the enolate anions of Chls are ambident nucleophiles that are of considerable organic chemical interest in relation to the theory of electron delocalization (aromaticity) and charge-transfer in large conjugated π-systems, as well as the chemical reactivity of such systems.[17] The examination of a detailed reaction mechanism was also found necessary in seeking a reasonable interpretation for the differences observed in the oxidation results. Further, we will describe in detail the separation and purification of the oxidation products by medium-pressure liquid chromatography (MPLC) on a semi-preparative sucrose column and by normal phase high-pressure liquid chromatography (NP-HPLC) on a silica column.[23,24] The products are thoroughly characterized using ^{1}H and ^{13}C NMR spectroscopy, electronic absorption spectroscopy (UV–vis) as well as electrospray ionization mass spectrometry (ESI-MS). To our knowledge, completely assigned ^{1}H and ^{13}C NMR spectra for 13^2(*S*)- and 13^2(*R*)-HO-Chl *b* have not been published before.[15,25–27]

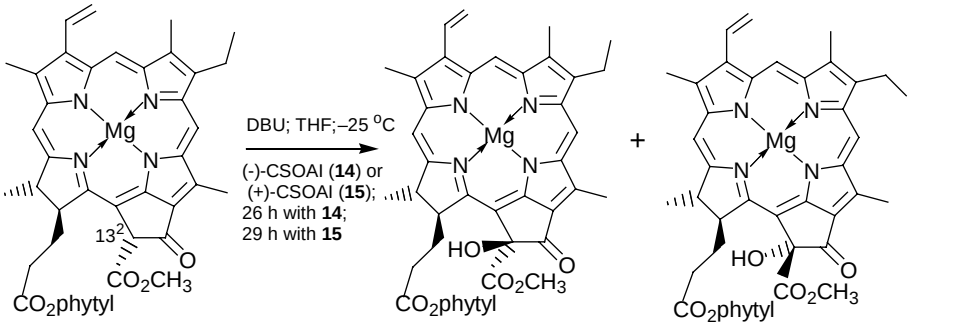

Scheme 1.

2. Results and discussion

2.1. Total yield and diastereoselectivity in the 13^2-hydroxylations of the chlorophylls with the (−)- and (+)-enantiomers of (10-camphorsulfonyl)oxaziridine

Under deaerated conditions, the (−)- and (+)-enantiomers of CSOAI are effective oxidants for the enolate anions of Chl *a* (**1**) and Chl *b* (**5**). The total yield of 13^2(*S*/*R*)-HO-Chl *a* (**3**/**4**) was 71 and 90% for the oxidations of Chl *a* with (−)-CSOAI (**14**) and (+)-CSOAI (**15**), respectively, (Scheme 1). These yields are of approximately the same magnitude but in reversed order as compared with those reported by Ma and Dolphin for the oxidations of pheophytin *a* (**9**) or methyl pheophorbide *a* (**10**).[20] We ascribe this noticeable difference in the yields to originate from the effect of the 6-coordinated central magnesium on the conformation and reactivity of Chl *a*. The macrocycle of pheophytin *a*–Mg(II)·2THF is likely to have a more planar and more rigid conformation as compared with the metal-free pheophytin *a*. Only negligible amounts of side-products, such as the 15^2-methyl, 17^3-phytyl ester of Mg-15^1(*S*/*R*)-unstable chlorin-7 (**16**) [Mg-3^1,3^2-didehydro-15^1,15^1-dihydroxy-rhodochlorin-15-acetic acid-15^1(*S*/*R*)-δ-lactone][9,23,28–33] was occasionally detected by UV–vis spectroscopy and by converting the lactone diastereomers with diazomethane[34] to the 13^1,15^2-dimethyl, 17^3-phytyl ester of Mg-purpurin-7 (**18**) [Mg-3^1,3^2-didehydro-rhodochlorin-15-glyoxylic acid].[9,23,28–30,33]

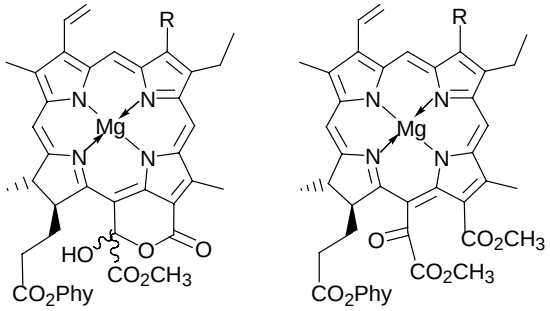

Under comparable reaction conditions, Chl *b*, however, clearly behaved differently from Chl *a*. The total yield of 13^2(*S*/*R*)-HO-Chl *b* (**7**/**8**) was 40% in the oxidation with (−)-CSOAI (**14**) and 60% in the reaction with (+)-CSOAI (**15**) (Scheme 2).

A competing side-reaction, which resulted in a very polar Chl *b* derivative, accounts largely for the lower yields of **7**/**8**. This polar Chl *b* derivative was identified as the 15^2-methyl, 17^3-phytyl ester of Mg-15^1(*S*/*R*)-unstable rhodin (**17**)

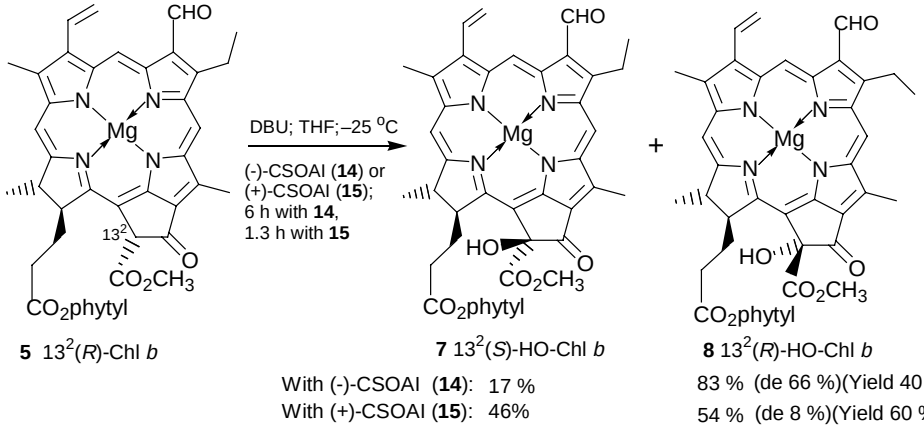

Scheme 2.

[Mg-3^1,3^2-didehydro-15^1,15^1-dihydroxy-7^1-oxo-rhodochlorin-15-acetic acid-15^1(*S*/*R*)-δ-lactone][15,28,29,31] on the basis of the UV–vis spectrum, ESI-MS and by converting the lactone diastereomers with diazomethane to the 13^1,15^2-dimethyl, 17^3-phytyl ester of Mg-7^1-oxo-purpurin-7 (**19**) [Mg-3^1,3^2-didehydro-7^1-oxo-rhodochlorin-15-glyoxylic acid].[15,28,29] The formation of the Mg-unstable rhodin side-products was largely avoided and the yield of 13^2(*S*/*R*)-HO-Chl *b* was improved by increasing the volume of hexane and using 0.1 M phosphate buffer, pH 5.5, instead of pure water in the first step of the work-up, that is, when washing the hexane solution of the reaction mixture for the first time.

The diastereoselectivity of each hydroxylation reaction was determined by NP-HPLC.[23,24] A complete resolution between the 13^2(*S*)- and 13^2(*R*)-diastereomers was achieved in each separation. The de was 94% for 13^2(*R*)-HO-Chl *a* (**4**) in the oxidation of Chl *a* (**1**) with (−)-CSOAI (**14**), but only 10% when (+)-CSOAI (**15**) was used as oxidant (Scheme 1, Fig. 1).

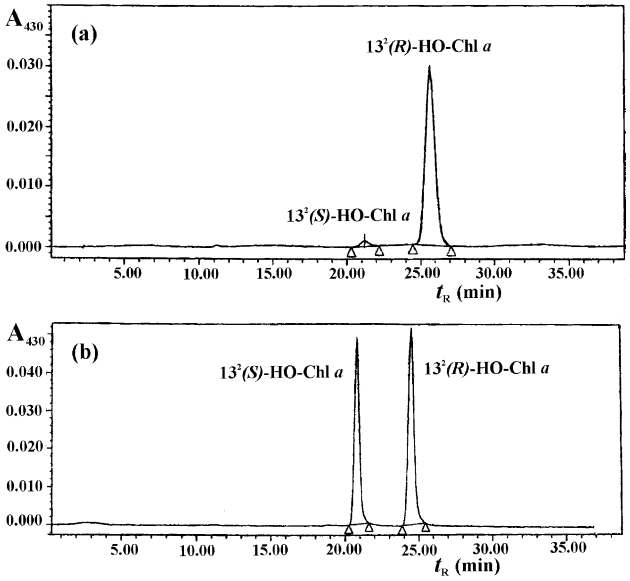

Figure 1. Normal-phase HPLC separation of 13^2(*S*)-HO-Chl *a* (**3**) and 13^2(*R*)-HO-Chl *a* (**4**) on the LiChrospher Si 60 column (250×4.0 mm i.d., 5 μm, Merck). Mobile phase: 1.0% (v/v) 2-PrOH in hexane. (a) Products obtained with (−)-CSOAI, (b) products obtained with (+)-CSOAI.

The oxidation of Chl *b* (**5**) with (−)-CSOAI and (+)-CSOAI resulted in a 66 and 8% de, respectively, in favour of 13^2(*R*)-HO-Chl *b* (**8**) (Scheme 2, Fig. 2). We seek to interpret the foregoing results regarding the total yield and diastereoselectivity by examining the detailed mechanism of the reactions.

2.2. Mechanism of the 13^2-hydroxylations of the chlorophylls with the (−)- and (+)-enantiomers of (10-camphorsulfonyl)oxaziridine

The (−)- and (+)-CSOAI (**14**,**15**) are effective oxidants of the Chl enolate anion (**20**, Scheme 3), produced from Chl as a result of C-13^2 deprotonation by DBU [pK_a (THF)=16.8; pK_{ip} (THF)=18.0 (subscript ip refers to a correction for ion-pairing using the Fuoss equation);[35,36] pK_a (acetonitrile)=24.0[37,38]]. The Chl enolate anion can be envisaged as

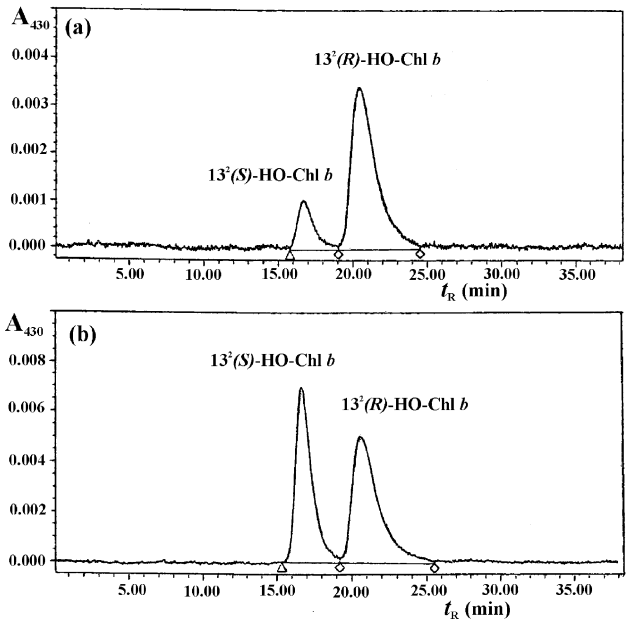

Figure 2. Normal-phase HPLC separation of 13^2(*S*)-HO-Chl *b* (**7**) and 13^2(*R*)-HO-Chl *b* (**8**) on the LiChrospher Si 60 column (250×4.0 mm i.d., 5 μm, Merck). Mobile phase: 2.0% (v/v) 2-PrOH in hexane. (a) Products obtained with (−)-CSOAI, (b) products obtained with (+)-CSOAI.

an ambident nucleophile (reviewed in Ref. 39, pp 322–325), which in the transition state of the reaction behaves as the C-13^2 carbanion, attacking the oxygen atom of the three-membered oxaziridine ring (Scheme 3).[18,39] The ring is opened while the bonding electron pair between O and N

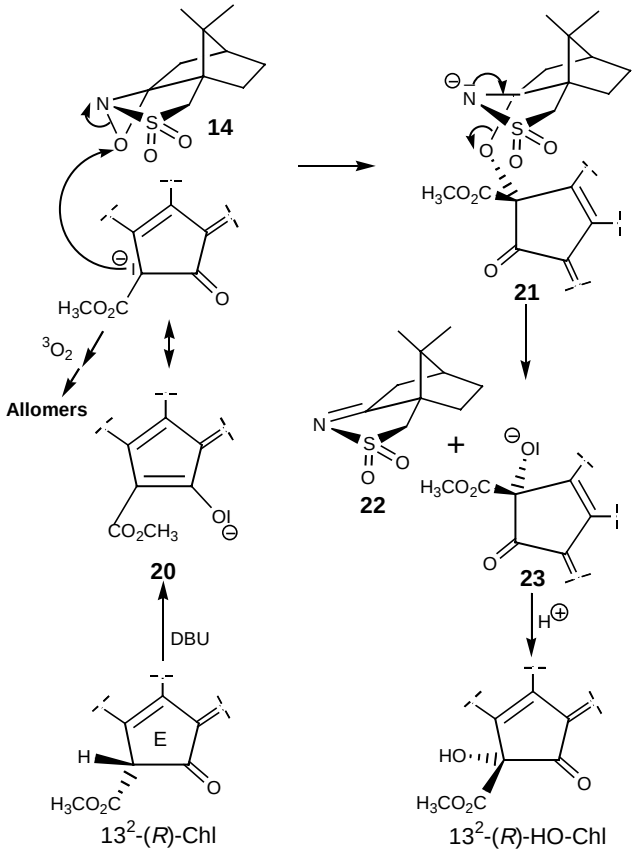

Scheme 3.

is transferred to the nitrogen atom. The resulting indermediate (**21**) disintegrates into the camphoryl-*N*-sulfate imine (**22**) and the 13^2-oxide anion of Chl (**23**). Protonation of the latter affords the final product, which is almost exclusively the $13^2(R)$-hydroxy-Chl, when (−)-CSOAI (**14**) is used as oxidant.

The diastereoselectivity, favouring the formation of $13^2(R)$-HO-Chl, especially with (−)-CSOAI (**14**), can be explained in terms of kinetic control, arising from steric hindrance, exerted by the 17-propionate phytyl ester group of the Chl enolate ion on the one hand and by the bulky camphorsulfonyl unit of the oxaziridines on the other hand. The highly space-demanding 17-propionate phytyl ester group, protruding over the front side of the isocyclic ring E, prevents the (−)-CSOAI oxidant from approaching the C-13^2 of the Chl enolate ion from the front side, but allows it to approach from the more open back side (*re*-face). This results in a moderate total yield of $13^2(S/R)$-HO-Chl, but high diastereomeric excess, favouring $13^2(R)$-HO-Chl as the prevailing diastereomer. The camphorsulfonyl unit of the (+)-enantiomer of CSOAI (**15**) causes less steric hindrance than the unit of the (−)-enantiomer (**14**). Consequently, (+)-CSOAI can approach the C-13^2 of the Chl enolate ion almost equally from either side. This results in a high total yield of $13^2(S/R)$-HO-Chl, but low diastereomeric excess, favouring only slightly $13^2(R)$-HO-Chl. In addition, it is noteworthy that the $13^2(R)$- and $13^2(S)$-diastereomers of 13^2-HO-Chl are not interconvertible (cf. thermodynamic control), because enolization in ring E is not possible in these Chl derivatives. Possible reasons for the different results of the Chl *a* and Chl *b* oxidations are discussed below.

2.3. Comparison of the ^{1}H and ^{13}C chemical shifts of the $13^2(S)$- and $13^2(R)$-diastereomers of 13^2-HO-Chl *a* (3/4) and 13^2-HO-Chl *b* (7/8)

Tables 1 and 2 present the ^{1}H and ^{13}C NMR δ-values for the $13^2(S)$- and $13^2(R)$-diastereomers of 13^2-HO-Chl *a* and 13^2-HO-Chl *b*. Comparison of the δ_H-values of $13^2(S)$-HO-Chl *a* and $13^2(R)$-HO-Chl *a* shows that the greatest differences occur for the 17-CH, 17^1-CH_2 (H_a, $H_{a'}$) and 17^2-CH_2 (H_b, $H_{b'}$) protons. These differences can be interpreted as arising from the conformational alterations occurring in the propionate phytyl ester side-chain and ring D as a result of the change of stereochemical configuration at C-13^2. However, the stereochemical alterations also induce small differences in the case of the methine-bridge 5-CH and 10-CH protons, as well as the 13^2-COH proton. The δ_H-values, 6.01 and 6.04, of the 13^2-COH proton, deserve special attention, because these values are very close to the corresponding values, 6.15 and 6.06, of $13^2(R)$-Chl *a* and $13^2(S)$-Chl *a*.[40] Hence, it would be very difficult to distinguish the 13^2-hydroxylated chlorophylls from the intact, naturally occurring chlorophylls solely on the basis of the ^{1}H NMR and UV–vis spectra; [the UV–vis spectra are identical for $13^2(S/R)$-HO-Chl *a* and $13^2(S/R)$-Chl *a* as well as for $13^2(S/R)$-HO-Chl *b* and $13^2(S/R)$-Chl *b*].

Inspecting next the differences in the δ_H-values between $13^2(S)$-HO-Chl *b* and $13^2(R)$-HO-Chl *b*, we observe that the differences are comparable to those in the *a*-series compounds. In the case of the *b*-series compounds, attention should be focused on the effect of the electron-withdrawing C-7 formyl group on the δ_H-values. As expected, there is a clear deshielding effect in the case of the 5-CH proton.

Table 1. ^{1}H NMR chemical shifts (δ_H, ppm, relative to Me_4Si in acetone-d_6) for $13^2(R)$-HO-Chl *a* (**4**), $13^2(S)$-HO-Chl *a* (**3**), $13^2(R)$-HO-Chl *b* (**8**) and $13^2(S)$-HO-Chl *b* (**7**)

Proton	Multiplicity, $^nJ_{H-H}$ (Hz)	**4**[a]	**3**[a]	**8**[b]	**7**[b]
2^1-CH_3	s	3.36	3.36	3.30	3.30
3^1-CH (H_X)	dd, $^3J_{cis}=11.6$, $^3J_{trans}=17.8$	8.14	8.14	8.30	8.30
3^2-CH_2 (H_{cis})	dd, $^2J_{gem}=1.5$, $^3J_{cis}=11.6$	6.02	6.02	6.04	6.04
3^2-CH_2 (H_{trans})	dd, $^2J_{gem}=1.5$, $^3J_{trans}=17.8$	6.23	6.23	6.28	6.28
5-CH	s	9.45	9.48	10.17	10.17
7^1-CH_3	s	3.31	3.31	—	—
7^1-CHO	s	—	—	11.20	11.20
8^1-CH_2	q, $^3J_{8^1-8^2}=7.6$	3.83	3.83	4.19	4.19
8^2-CH_3	t, $^3J_{8^1-8^2}=7.6$	1.72	1.71	1.79	1.79
10-CH	s	9.78	9.80	9.92	9.92
12^1-CH_3	s	3.64	3.64	3.62	3.62
13^2-COH	s	6.01	6.04	6.12	6.16
13^4-CH_3	s	3.61	3.59	3.60	3.60
17-CH	m	4.66	4.16	4.63	4.08
17^1-CH_2 ($H_{a'}$)	m	2.20[c]	2.85[c]	2.20[c]	2.30[c]
17^1-CH_2 (H_a)	m	2.20[c]	2.57[c]	2.20[c]	2.10[c]
17^2-CH_2 ($H_{b'}$)	m	2.37[c]	2.43[c]	2.37[c]	2.50[c]
17^2-CH_2 (H_b)	m	1.90[c]	2.06[c]	1.90[c]	2.20[c]
18-CH	dq, $^3J_{18-18^1}=7.3$	4.55	4.55	4.50	4.49
18^1-CH_3	d, $^3J_{18-18^1}=7.3$	1.65	1.57	1.64	1.64
20-CH	s	8.62	8.62	8.52	8.49
P1–CH_2 (H_a)	d/m, $^3J_{P2-P1}=7.1$	4.44	4.45	4.42	4.42
P1–CH_2 (H_b)	d/m, $^3J_{P2-P1}=7.1$	4.44	4.49	4.42	4.42
P2–CH	tq, $^3J_{P2-P1}=7.1$	5.16	5.17	5.13	5.24
$P3^1$–CH_3	s	1.57	1.60	1.55	1.55
P4–CH_2[d]	m	1.90	1.90	1.87	1.87

[a] Values consistent with those published earlier in Ref. 24.
[b] Values measured on a Bruker Avance spectrometer, ν (^{1}H)=500 MHz.
[c] Requires spin simulation for the fragment 17-CH–17^1-CH_2–17^2-CH_2.
[d] The P5–P16 part of the phytyl group spectrum was as reported in Ref. 46.

Table 2. Broad-band proton decoupled ^{13}C NMR chemical shifts (δ_C, ppm, relative to Me_4Si in acetone-d_6) for $13^2(R)$-HO-Chl *a* (**4**), $13^2(S)$-HO-Chl *a* (**3**), $13^2(R)$-HO-Chl *b* (**8**) and $13^2(S)$-HO-Chl *b* (**7**).

Carbon	**4**[a]	**3**[a]	**8**[b]	**7**[b]
1	155.51	155.54	157.43	157.52
2	136.07	136.11	136.94	136.84
2^1	12.54	12.55	12.39	12.39
3	139.93	139.97	141.08	141.08
3^1	131.37	131.37	130.87	130.85
3^2	120.19	120.29	120.85	120.81
4	148.75	148.70	149.74	149.80
5	100.94	101.05	104.15	104.22
6	152.53	152.44	149.20[c]	149.37[c]
7	134.71	134.84	131.59	131.62
7^1	11.14	11.14	188.47	188.48
8	144.87	144.97	155.77	155.64
8^1	19.98	19.96	19.75	19.57
8^2	18.01	18.02	19.56	19.39
9	146.87	146.87	143.49	143.59
10	108.09	108.21	111.03	111.11
11	148.33	148.42	149.16[c]	149.25[c]
12	134.98	134.75	139.26	138.85
12^1	12.74	12.71	12.82	12.79
13	129.29	129.74	130.54	130.53
13^1	192.80	193.04	193.38	193.48
13^2	90.77	90.75	90.68	90.50
13^3	174.66	174.09	174.44	173.78
13^4	53.29	53.04	53.42	53.17
14	162.42	162.27	163.83	163.85
15	109.28	109.12	109.15	108.86
16	157.61	158.23	160.42	161.37
17	50.30	51.91	50.36	52.19
17^1	31.30	32.17	31.02[d]	32.20[d]
17^2	31.10	31.27	30.97[d]	31.62[d]
17^3	173.40	173.69	173.32	173.75
18	50.40	49.81	50.31	49.73
18^1	23.39	23.36	23.32	23.32
19	169.95	169.85	171.70	171.63
20	94.04	94.23	94.22	94.39
P1	61.41	61.42	61.43	61.55
P2	119.32	119.48	119.30	119.57
P3	142.67	142.52	142.79	141.08
$P3^1$	16.22	16.24	16.21	16.31
P4[e]	40.30	40.34	40.30	40.40

[a] Values consistent with those published earlier in Ref. 24.
[b] Values measured on a Bruker Avance spectrometer, ν (^{13}C)=125 MHz.
[c] The assignments of carbons 6 and 11 are interchangeable.
[d] The assignments of carbons 17^1 and 17^2 are interchangeable.
[e] The P5–P16 part of the phytyl group spectrum was as reported in Ref. 46.

The 8^1-CH_2, 10-CH, and 13^2-COH protons also exhibit deshielding, but the effect is attenuated the farther the proton is located from the formyl group.

Comparison of the differences in the δ_C-values (Table 2) between $13^2(S)$-HO-Chl *a* and $13^2(R)$-HO-Chl *a* as well as those between $13^2(S)$-HO-Chl *b* and $13^2(R)$-HO-Chl *b*, indicates that the change of stereochemical configuration at C-13^2 induces only slight differences in the values both in the *a*-series and the *b*-series compounds. Of special interest are the δ_C-values of C-13^2, which are at ca. 91 ppm for the diastereomers of both series. This carbon is deshielded by approximately 25 ppm relative to the C-13^2 of $13^2(R)$-Chl *a* (δ_C=65.5).[24] Owing to this, ^{13}C NMR spectroscopy is a good method to distinguish the 13^2-hydroxylated chlorophylls from the intact, naturally occurring chlorophylls.

In addition, ^{13}C NMR spectroscopy is expected to give valuable information regarding the effect of the electron-withdrawing C-7 formyl group on the electron densities of the macrocyclic carbons. Inspection of the δ_C-values in Table 2 shows that most macrocyclic carbons of $13^2(S/R)$-HO-Chl *b* experience deshielding relative to the corresponding carbons of $13^2(S/R)$-HO-Chl *a*. The deshielding effect is attenuated the farther the carbon is located from the formyl group. However, carbons 6 and 9 represent a clear exception to this rule. Contrary to expectations, these carbons are shielded by ca. 3 ppm relative to the *a*-series compounds.

2.4. Possible reasons for the different results of the Chl *a* and Chl *b* oxidations

A conspicuous feature in the foregoing synthesis results is the outcome of the Chl *b* oxidations, which is clearly different from that of the Chl *a* oxidations, despite the use of comparable reaction conditions in both oxidations. In particular, when Chl *b* was oxidized with (−)-CSOAI, the total yield of $13^2(S/R)$-HO-Chl *b* (**7/8**) remained quite modest (40%) and also the diastereoselectivity (de 66%) was clearly lower than that (de 94%) achieved in the corresponding Chl *a* oxidation. In seeking a reasonable interpretation for the different outcome of the Chl *b* oxidations, we will first consider the possibility of the formation of the Mg-$15^1(S/R)$-unstable rhodin side-products (**17**) in the reaction mixture during the reaction period.

The side-products **17** and $13^2(S/R)$-HO-Chl *b* might both be formed in the reaction mixture via the allomerization reaction, if some adventitious ground-state (triplet) oxygen and water remained in the mixture in spite of the careful deaeration and drying procedures of the reagent solutions (cf. Section 4). Being very reactive with the enolate anion of Chl *b* (**20**, Scheme 3), the triplet oxygen would be kinetically capable of competing with CSOAI and initiating the free-radical allomerization (FRA),[16] which, in the presence of water/hydroxide ion, would be expected to yield $13^2(S/R)$-HO-Chl *b* and the Mg-$15^1(S/R)$-unstable rhodin products **17** from Chl *b*. As Chl *b* is more difficult to dehydrate than Chl *a*, it is possible that an equimolar amount of water was introduced with Chl *b* into the reaction mixture, where the H_2O was deprotonated by DBU (a strong base, but a weak nucleophile) to give the HO^- ion. Being a strong base and a strong nucleophile, the latter is probably capable of reacting with the oxaziridine ring of the (−)- or (+)-enantiomer of CSOAI, thus reducing the concentration of the reactive oxidant in the desired reaction. However, it is also possible that the strongly electron-withdrawing effect of the C-7 formyl group of the Chl *b* enolate anion was mediated down to the isocyclic ring E,[17] thereby reducing the nucleophilicity of the Chl *b* enolate anion and the probability of its desired oxidation by CSOAI. Furthermore, the conformational alterations, induced by the electron-withdrawing C-7 formyl group in the reduced sub-ring D and the C-17 propionate phytyl ester group,[17] are likely to influence the oxidation results of Chl *b*.

In trying to estimate the possibility of the second alternative, that is, that the side-products **17** were formed, when the reaction mixture was poured into the hexane/water partition system, it is noteworthy that a minor part of $13^2(S/R)$-HO-Chl *b* and presumably all of the side-products **17** went into the aqueous phase and were lost, because this phase was discarded (cf. Section 4). It is possible that these

allomerization products were formed from some unreacted Chl *b* enolate anion in the first partition step of the work-up, where plenty of triplet oxygen, water and presumably also hydroxide ion were present. Further, it seems also possible that the strongly basic conditions hindered protonation of the Chl *b* 13^2-oxide anion (**23**, Scheme 3), which, due to its negative charge, would be distributed largely into the aqueous phase of the first hexane/water partition system. Such a hindrance would explain why a noticeable part of 13^2-HO-Chl *b* was found in the water phase, because the negative charge of its anion would make it highly soluble in water. This interpretation is supported by the observation that the formation of the side-products **17** was largely avoided and the yield of 13^2(*S*/*R*)-HO-Chl *b* was improved by increasing the volume of hexane and using 0.1 M phosphate buffer, pH 5.5, instead of water in the first washing of the hexane solution of the reaction mixture [cf. the synthesis of 13^2(*S*/*R*)-HO-Chl *b* with (+)-CSOAI]. These changes in the work-up also seemed to lessen the difficulty encountered in the handling of the polar Chl *b* derivatives, which had a high tendency to form aggregates and emulsions on equilibrating the hexane phase with water in the work-up.

3. Conclusions

The results obtained verify that the use of the sterically hindered reagents, (−)- or (+)-CSOAI (oxidant) and DBU (base), results in a high total yield of 13^2(*S*/*R*)-HO-Chl *a* or 13^2(*S*/*R*)-HO-Chl *b*, starting from 13^2(*R*)-Chl *a* or -Chl *b*, respectively. Owing to steric factors, a high diastereoselectivity is also achieved using (−)-CSOAI, which affords 13^2(*R*)-HO-Chl as the prevailing diastereomer. The mechanism of the reactions involves the formation of the Chl enolate anion, which can be envisaged as an ambident nucleophile, attacking, in the transition state of the reaction, as the 13^2-carbanion the oxygen atom of the oxaziridine ring of CSOAI. Several factors were found possible to explain the differences observed in the oxidation results of Chl *a* and Chl *b*. The synthesis procedures described in this article represent the best methods so far developed for the preparation 13^2(*S*/*R*)-hydroxychlorophylls *a* and *b*, both regarding the regioselectivity and the stereoselectivity of the reactions.

4. Experimental

4.1. Reagents, solvents and preparation of Chl *a* (1) and Chl *b* (5)

(1*R*)-(−)-(10-Camphorsulfonyl)oxaziridine (98%), (1*S*)-(+)-(10-camphorsulfonyl)oxaziridine (98%), and 1,8-diazabicyclo[5.4.0]undec-7-ene, DBU (98%) were purchased from Aldrich and used without further purification. Et_2O (dried, stabilized with butylated hydroxytoluene, BHT), 1-PrOH, and 2-PrOH were of Merck's analytical grade purity and were used as provided, unless otherwise stated. THF (Merck, analytical grade, stabilized with BHT) was dried with Na wire and distilled just before use. Hexane (LabScan, HPLC grade) was distilled through a Vigreux column. Chloroform (Merck, LiChrosolv, stabilized with amylene) was dried with silica gel.

Chl *a* and Chl *b* were isolated from clover leaves by the method described earlier,[41] but since then modified for large-scale preparation.[42] The purity of each chlorophyll preparation was ascertained by electronic absorption spectra,[43] ^{1}H NMR spectra,[43] TLC on sucrose,[44] and NP-HPLC.[23] The spectroscopic properties of the preparations were identical with those described previously.[43] The ^{1}H NMR spectra showed water as the only impurity (present in a ratio smaller than 1:1). The sucrose TLC with fluorescence detection under UV light (λ=366 nm) and NP-HPLC revealed trace amounts of Chl *a*′ (13^2(*S*)-Chl *a*] and pheophytin *a* in the Chl *a* preparation, and a small amount (<1%) of Chl *b*′ in the Chl *b* preparation.

4.2. Synthesis of 13^2(*S*/*R*)-hydroxychlorophylls *a* and *b*

4.2.1. Diastereoselective synthesis of 13^2(*R*)-hydroxychlorophyll *a* (4) with (−)-CSOAI (14). Solid 13^2(*R*)-Chl *a* (**1**) (20 mg, 0.22×10^{-4} mol) was weighed into a dry two-necked reaction flask (25 mL; the middle-neck was provided with a two-way stopcock, one way of which was connected to a vacuum pump and the other way to an argon balloon; the side-neck was provided with a septum) and dissolved in dry THF (10 mL). The solution was deaerated applying the freeze-pump-thaw technique with three cycles, after which an argon atmosphere was let to flow into the reaction flask. In another two-necked flask, (−)-CSOAI (**14**) (6.2 mg, 0.27×10^{-4} mol) was dissolved in THF (5.0 mL). DBU (3.5 mL, 0.022 mol) was measured into a third two-necked flask. Applying the freeze-pump-thaw technique, air was removed from both flasks and replaced with argon. Then the Chl *a* solution in the reaction vessel was cooled to a temperature of −25 °C on a bath consisting of a mixture of solid CO_2 and CCl_4, and vigorous magnetic stirring of the solution was started. The DBU solution at room temperature was withdrawn with a syringe through the septum from its flask and injected slowly into the reaction vessel. No clear change in the colour of the mixture (dark green) was observed on the addition of the base. After 15 min, the THF solution of (−)-CSOAI (**14**) was withdrawn with a syringe through the septum from its flask and injected into the reaction mixture. The progress of the reaction was followed by taking 0.1 mL aliquots of the reaction mixture, which were analyzed by TLC on sucrose (eluent: 1-PrOH/hexane, 1:99, w/w).[44] For TLC, hexane (3 mL) was added to each aliquot in a small separatory funnel and the solution was washed with distilled water (3×15 mL). The hexane solution was evaporated to dryness in a small tube with the aid of an argon stream, the residue dissolved in a suitable volume of Et_2O, and the solution applied with a capillary onto a sucrose TLC plate. After development, the components on the chromatogram were identified by comparing the R_f-values with those reported by Sahlberg and Hynninen.[44] As the reaction was not complete after 4 h, the reaction vessel was placed into a freezer (−20 °C) and kept overnight, without stirring. After 26 h, only a few percent of Chl *a* was left and, therefore the reaction was terminated by pouring the mixture into 80 mL of hexane in a separatory funnel. The hexane solution was washed with distilled water (3×150 mL) to remove all

water-soluble components. Judging from the pale wash water, only small amounts of dephytylated, water-soluble Chl derivatives, such as chlorophyllide, pheophorbide, and their hydroxylated derivatives, were formed in the reaction. The washed hexane solution of the products was evaporated to dryness at reduced pressure by a rotary evaporator.

The oxidation products were purified by MPLC on a semi-preparative sucrose column. The sample for chromatography was prepared by dissolving the residue in the rotary evaporator flask in 2 mL of Et_2O and adding 8 mL of the eluent (THF/2-PrOH/hexane, 0.5:1.0:98.5, w/w/w) to the solution. Isocratic elution resolved the main products as a separate zone from the two faster migrating zones, containing non-reacted Chl *a* and its $13^2(S)$-epimer, Chl *a*′. The combined fractions of each zone were evaporated to dryness by a rotary evaporator and the possible small amount of water removed from the samples by chloroform co-distillation (three times).[23] The residual solvents were removed from the samples on a vacuum line (0.01 mbar). The yield of the main product, 13^2-HO-Chl *a*, was 14.5 mg (71%) and that of Chl *a* and Chl *a*′ 3.6 mg (18%). The spectrometric data of the main product (^{1}H and ^{13}C NMR spectra, UV–vis spectrum, and ESI-MS) were consistent with the structural data published earlier for $13^2(R)$-HO-Chl *a*.[24] The $13^2(S)$- and $13^2(R)$-diastereomers of HO-Chl *a* were only partially resolved from one another by MPLC on the sucrose column, but were completely resolved by NP-HPLC. A 94% diastereomeric excess for $13^2(R)$-HO-Chl *a* was obtained by NP-HPLC (Fig. 1a).

4.2.2. Synthesis of $13^2(S/R)$-hydroxychlorophyll *a* (3/4) with (+)-CSOAI (15). The synthesis procedure was nearly equivalent to that used in the diastereoselective synthesis of $13^2(R)$-HO-Chl *a*. Some differences were, however, introduced. The amounts of reagents and THF were doubled and (−)-CSOAI (**14**) was replaced with (+)-CSOAI (**15**). The addition of DBU into the reaction flask (50 mL) turned instantly the dark green colour of the reaction mixture reddish, indicating the formation of the Chl enolate anion. The (+)-CSOAI, dissolved in THF (10 mL), was injected into the reaction mixture after 5 min from the addition of DBU while the temperature stayed at −25 °C. The reaction was monitored by sucrose–TLC with THF/2-PrOH/hexane (0.5:2.0:97.5, w/w/w) as eluent. This more polar eluent resolved the $13^2(S)$- and $13^2(R)$-diastereomers of HO-Chl *a* into two separate spots. As the reaction was not complete after 8 h, the reaction flask was placed into a freezer (−20 °C) for 15 h. After a total reaction time of 29 h, only a trace of Chl *a* was observed on the sucrose TLC plate under UV-light by fluorescence emission. Hence, the reaction mixture was poured into 200 mL of hexane in a separatory funnel and the hexane phase was washed with distilled water (6×330 mL).

The oxidation products were purified by MPLC on a semi-preparative sucrose column. The sample for chromatography was prepared by evaporating the hexane solution of the products to near dryness, dissolving the residue in the rotary evaporator flask in 4.0 mL of Et_2O and adding 16 mL of the eluent (THF/2-PrOH/hexane, 0.5:1.0:98.5, w/w/w) to the solution. Isocratic elution resolved the main products as a separate zone from the faster migrating two zones, containing the non-reacted Chl *a* and its $13^2(S)$-epimer, Chl *a*′. The $13^2(S/R)$-HO-Chl *a* zone was followed by a small amount (ca. 1 mg) of a bluish component, identified as the 15^2-methyl, 17^3-phytyl ester of Mg-unstable chlorin-7 (**16**) [Mg-3^1,3^2-didehydro-15^1,15^1-dihydroxy-rhodochlorin-15-acetic acid-15^1(*S*/*R*)-δ-lactone],[9,23,28–33] on the basis of the UV–vis spectrum, λ_{max} in Et_2O at 651.5 (0.474), 605 (0.074), 562 (0.036), 519 (0.032), 483 (0.018), 417.0 (1.000) nm, and by converting the lactone diastereomers with diazomethane to the 13^1,15^2-dimethyl, 17^3-phytyl ester of Mg-purpurin-7 (**18**) [Mg-3^1,3^2-didehydro-rhodochlorin-15-glyoxylic acid];[9,23,28–30,33] UV–vis spectrum: λ_{max} in Et_2O at 669.0 (0.394), 572 (0.088), 525 (0.038), 495 (0.025), 422.0 (1.000) nm.

Only traces of immobile pigments were retained in the pre-column. The combined effluent fractions of each zone were evaporated to dryness at reduced pressure and the possible small amount of water removed from the samples by chloroform co-distillation (three times). The residual solvents were removed from the samples on a vacuum line (0.01 mbar). The yield of the main products, $13^2(S/R)$-HO-Chl *a*, was 38.4 mg (90%) and that of Chl *a* and Chl *a*′ 2 mg (5%). A 10% diastereomeric excess for $13^2(R)$-HO-Chl *a* was obtained by NP-HPLC (Fig. 1b). The spectrometric data of the main products (^{1}H and ^{13}C NMR spectra, UV–vis spectrum, and ESI-MS) were consistent with the structural data published earlier for $13^2(S)$- and $13^2(R)$-HO-Chl *a*.[24] The ^{1}H and ^{13}C NMR assignments for **3** and **4** appear from Tables 1 and 2. ESI-MS: *m*/*z* 909.4 $(M+1)^+$; $C_{55}H_{72}N_4O_5Mg$ requires 908.5. UV–vis spectrum in Et_2O: λ_{max} at 661.6 (0.847), 614.5 (0.139), 573.5 (0.076), 530.3 (0.043), 429.3 (1.000) and 410.9 (sh, 0.761) nm.

4.2.3. Diastereoselective synthesis of $13^2(R)$-hydroxychlorophyll *b* (8) with (−)-CSOAI (14). The synthesis procedure corresponded to that used in the diastereoselective synthesis of $13^2(R)$-HO-Chl *a*, but double amounts of reagents were now used. $13^2(R)$-Chl *b* (**5**) (40.5 mg, 0.45×10^{-4} mol) was weighed into the reaction flask (50 mL) and dissolved in THF (20 mL). The addition of DBU (6.8 mL, 0.045 mol) to the solution immediately turned the dark green Chl *b* solution dark brown, indicating the formation of the Chl *b* enolate anion. Enolization seemed to occur more rapidly for Chl *b* than for Chl *a*. After 10 min, (−)-CSOAI (**14**) (12.2 mg, 0.53×10^{-4} mol) in THF (10 mL) was added to the solution at −25 °C. Monitoring of the reaction by sucrose TLC (eluent: 1-PrOH/hexane, 1.0:99.0, w/w) indicated that, after ca. 5 h from the addition of the oxidant, all of the original Chl *b* had reacted. Hence, after 6 h, the reaction mixture was poured into 350 mL of hexane and 1000 mL of water in a separatory funnel. On equilibrating the phases, a major part of the green pigments was distributed into the hexane phase, while a minor part went into the water phase. The partition work-up was hampered by the strong aptitude of the polar Chl *b* derivatives to form aggregates and emulsions. The hexane phase (ca. 350 mL) was washed with distilled water (2×1000 mL) and evaporated to dryness at reduced pressure. The products in the residue were purified by MPLC on a semi-preparative sucrose column (eluent: THF/2-PrOH/hexane, 0.5:1.0:98.5, w/w/w). The sample was prepared by dissolving the residue in the evaporator flask in 4 mL of Et_2O, to which 16 mL of the eluent was

added. In the MPLC, the aggregated and very polar pigments behaved as an immobile green material, firmly adsorbed on the sucrose of the pre-column. The 13^2(*S*)- and 13^2(*R*)-diastereomers of HO-Chl *b* were only partially resolved from one another by MPLC on the sucrose column. After high-vacuum treatment, their total yield was 16.6 mg (40%). The diastereomers (**7/8**) were completely resolved by NP-HPLC (Fig. 2a). A 66% diastereomeric excess for 13^2(*R*)-HO-Chl *b* was obtained by NP-HPLC (Fig. 2a).

The green pigments, distributed into the water phase, were discarded after they were analyzed by TLC on sucrose (eluent: 1-PrOH/hexane, 1.0:99.0, w/w). For TLC, the pigments were salted out with NaCl into Et_2O (LabScan) from the water phase. The TLC results showed that the water phase contained 13^2-HO-Chl *b* (ca. 80% of the water-phase pigments) and a very polar Chl *b* derivative (ca. 20%). The latter was identified as the Mg-15^1(*S/R*)-HO-lactone **17** from Chl *b*, that is, the 15^2-methyl, 17^3-phytyl ester of Mg-unstable rhodin [Mg-3^1,3^2-didehydro-15^1,15^1-dihydroxy-7^1-oxo-rhodochlorin-15-acetic acid-15^1(*S/R*)-δ-lactone] [15,28,29,31] on the basis of the UV–vis spectrum, [λ_{max} in Et_2O at 630.0 (0.218), 584 (0.055), 535 (0.037), 443.0 (1.000) nm] and ESI-MS [$(M+1)^+$ at *m/z* 939.6; $C_{55}H_{70}N_4O_8Mg$ requires 938.5], and by converting the lactone diastereomers with diazomethane to the 13^1,15^2-dimethyl, 17^3-phytyl ester of Mg-*b*-purpurin-7 (**19**) [Mg-3^1,3^2-didehydro-7^1-oxo-rhodochlorin-15-glyoxylic acid];[15,28,29] UV–vis spectrum: λ_{max} in Et_2O at 639.0 (0.154), 535 (0.037), 447.0 (1.000) nm. The identification of the latter compound was confirmed by co-elution with an authentic compound[15] on a sucrose TLC plate. As shown below, the yield of 13^2(*S/R*)-HO-Chl *b* can be improved by increasing the volume of hexane in the work-up and by using 0.1 M phosphate buffer, pH 5.5, instead of pure water when washing the hexane solution of the reaction mixture for the first time.

4.2.4. Synthesis of 13^2(*S/R*)-hydroxychlorophyll *b* (7/8) with (+)-CSOAI (15). As in the preceding cases, the synthesis was carried out at −25 °C under an argon atmosphere. 13^2(*R*)-Chl *b* (**5**) (32.9 mg, 0.36×10^{-4} mol) was weighed into the reaction flask (50 mL) and dissolved in THF (17 mL). The addition of DBU (4.3 mL, 0.029 mol) to the solution immediately turned the dark green Chl *b* solution dark brown, indicating the formation of the Chl *b* enolate ion. After 3 min, (+)-CSOAI (**15**) (10 mg, 0.44×10^{-4} mol) in THF (10 mL) was added to the solution. With 0.029 mol of DBU, the oxidation seemed to take place fast. Therefore, the reaction mixture was poured after 1 h 18 min into a separatory funnel, containing 500 mL of hexane and 500 mL of 0.1 M phosphate buffer, pH 5.5. The partial distribution of 13^2(*S/R*)-HO-Chl *b* into the water phase and the formation of the Mg-unstable rhodin side-products **17** was largely avoided by increasing the volume of hexane and using the phosphate buffer when washing the hexane solution of the products for the first time. In the second and third washings, distilled water was used. After the washings, the hexane solution was evaporated to dryness at reduced pressure. The products in the residue were purified by MPLC on a semi-preparative sucrose column (eluent: THF/2-PrOH/hexane, 0.5:1.0:98.5, w/w/w). The sample was prepared by dissolving the residue in the evaporator flask in 4 mL of Et_2O+3 mL of THF +25 mL of the eluent. The 13^2(*S*)- and 13^2(*R*)-diastereomers of HO-Chl *b* were only partially resolved from one another by MPLC on the sucrose column. After high-vacuum treatment, their total yield was 20.1 mg (60%). The diastereomers (**7/8**) were completely resolved by NP-HPLC (Fig. 2b). An 8% diastereomeric excess for 13^2(*R*)-HO-Chl *b* was obtained by NP-HPLC (Fig. 2b). The ^{1}H and ^{13}C NMR assignments for **7** and **8** appear from Tables 1 and 2. ESI-MS: *m/z* 923.6 $(M+1)^+$; $C_{55}H_{70}N_4O_7Mg$ requires 922.5. UV–vis spectrum in Et_2O: λ_{max} at 642.5 (0.360), 593.6 (0.067), 566.0 (0.047), 452.1 (1.000) and 429.1 (sh, 0.335) nm.

4.3. Semi-preparative MPLC separations on a sucrose column

The semi-preparative MPLC separations of the Chl derivatives on a sucrose column were carried out using an equipment composed of a pump (Büchi 688), a separation column (Büchi 685, height 500 mm, i.d. 35 mm), a pre-column (Büchi, height 150 mm, i.d. 10 mm), and an argon-pressured feeding column for samples (Büchi). The separation column was packed with powdered sugar (Finnsugar Ltd, Suomen Sokeri Oy, FI-02460 Kantvik, Finland), having the following properties: mean particle size 0.035 mm, sucrose 98.4%, water 0.10%, tricalcium phosphate 1.5% and sulfur dioxide max. 10 mg/kg. The sugar was passed through a 180 μm sieve and mixed with hexane to form a suitable suspension, which was poured into the column. The sugar was allowed to settle while occasionally rotating the column in an upright position clockwise and counterclockwise about its long axis. The layer was made compact by pumping eluent through it until no settling movement was observed (pump pressure was then 20 bar). The separation column was packed up to the top of the column so that there was no void volume above the sugar layer. The use of the pre-column, which was packed in a similar fashion, proved important, because it retained the aggregated and very polar impurities of the Chl samples, preventing the impurities from spreading into the main sugar column. Thus, there was no need to repack the main column for every new separation; one only had to repack the pre-column. This enabled us to perform even 15 separations with the same sugar packing in the main column. The flowing rate of liquid in the separations was 2–10 mL/min, corresponding to the pump pressure of 2–15 bar. A rise in the pump pressure indicated obstruction of the sugar layer. THF–2-PrOH–hexane was used as eluent, varying the ratio of the solvent components in different separations. To avoid aggregation of Chl derivatives in the feeding procedure, the solvent for the sample to be fed had to be more polar than the eluent.

4.4. High-performance liquid chromatography

The use of semi-preparative and analytical NP-HPLC silica columns has been previously described by our group to separate various oxidation products of chlorophylls *a* and *b*.[15,23,24] The silica column, LiChrospher Si 60 (250×4.0 mm, 5 μm, Merck), was employed in this work to determine the de for the synthesis products. A complete resolution between the 13^2(*S*)- and 13^2(*R*)-diastereomers of HO-Chl *a* was achieved using 2-PrOH/hexane, 1.0:99.0,

v/v, as eluent (Fig. 1). The same solvent system with a higher proportion of the polar solvent, that is, 2-PrOH/hexane, 2.0:98, v/v, resolved completely the $13^2(S)$- and $13^2(R)$-diastereomers of HO-Chl *b* (Fig. 2). The solvent system for each 13^2-HO-Chl sample (THF/hexane, 10:90, v/v) had to be more polar than the eluent to avoid aggregation of the sample in the beginning of the separation. A 20 μL volume of a dilute solution of each 13^2-HO-Chl sample was injected into the apparatus. The flowing rate of the eluent was 1.0 mL min^{-1}. Absorbance of the effluent was monitored at 430 nm and the relative amounts of the diastereomers were obtained by integrating the concentration zones. The $13^2(R)$-diastereomer of HO-Chl *a* or HO-Chl *b*, completely characterized by NMR, served as an internal standard to determine the mutual order of the $13^2(S)$-and $13^2(R)$-diastereomers.

4.5. Spectrometric characterization of the products

We aimed at obtaining completely assigned ^1H and ^{13}C NMR spectra (Tables 1 and 2) for the $13^2(S)$- and $13^2(R)$-diastereomers of 13^2-HO-Chl *a* and 13^2-HO-Chl *b*, utilizing the two-dimensional (2D) techniques, ^1H,^{13}C HSQC and ^1H,^{13}C HMBC.[24,45,46] The 200 MHz ^1H NMR spectra were recorded on a Varian Gemini FT spectrometer. The 500 MHz ^1H, 125 MHz $^{13}C\{^1H\}$, 1D NOE, and 2D heteronuclear correlation NMR spectra were measured at room temperature on a Bruker Avance FT spectrometer. The NMR sample was prepared by dissolving in a 0.5 mm NMR tube 7–16 mg of purified Chl derivative in 0.7 mL of acetone-d_6 (ampoules from Fluka, 0.7 mL, *d*% 99.95, or from Euriso-Top, 0.75 mL, *d*% 99.8). The 1D NOE method[47,48] was used to determine the stereochemical configuration at C-13^2. For the $13^2(R)$-diastereomer, the NOE experiment showed correlations between the 13^4-CH_3 protons and the 17^1-CH_2/17^2-CH_2 protons, as well as between the 13^2-COH proton and the 17-CH proton, implying that these proton groups were spatially close to one another. In the case of the $13^2(S)$-diastereomer, such correlations could not be observed. The mass spectra were measured on a Mariner time-of-flight (TOF) mass spectrometer (PerSeptive Biosystems, Framingham, MA), using the positive-mode electrospray ionization (ESI), as described previously.[16] The electronic absorption spectra (UV–vis) were recorded on a Varian Cary 5E UV–vis–NIR spectrophotometer. The samples were dissolved in Et_2O (Merck, analytical grade, SeccoSolv).

Acknowledgements

We thank Dr. Kristiina Hyvärinen for helping us to carry out the normal-phase HPLC separations.

References and notes

1. Hynninen, P. H.; Leppäkases, T. S. The Functions of Chlorophylls in Photosynthesis. In *Encyclopedia of Life Support Systems (EOLSS)*; Hänninen, O. O. P., Atalay, M., Eds.; EOLSS: Oxford, UK, 2004; Developed under the auspices of the UNESCO; http://www.eolss.net.
2. Deisenhofer, J., Norris, J. R., Eds.; *The Photosynthetic Reaction Center*; Academic: New York, 1993; Vols. 1 and 2.
3. Liu, Z.; Yan, H.; Wang, K.; Kuang, T.; Zhang, J.; Gui, L.; An, X.; Chang, W. *Nature* **2004**, *428*, 287–292.
4. Jordan, P.; Fromme, P.; Witt, H. T.; Klukas, O.; Saenger, W.; Krauss, N. *Nature* **2001**, *411*, 909–917.
5. Ferreira, K. N.; Iverson, T. M.; Maghlaoui, K.; Barber, J.; Iwata, S. *Science* **2004**, *303*, 1831–1838.
6. Schoch, S.; Rüdiger, W.; Lüthy, B.; Matile, Ph. *J. Plant Physiol.* **1984**, *115*, 85–89.
7. Seely, G. R. The Structure and Chemistry of Functional Groups. In *The Chlorophylls*; Vernon, L. P., Seely, G. R., Eds.; Academic: New York and London, 1966; pp 67–109.
8. Jackson, A. H. Structure, Properties, and Distribution of Chlorophylls. In *Chemistry and Biochemistry of Plant Pigments*, 2nd ed.; Goodwin, T. W., Ed.; Academic: London, 1975; Vol. 1, pp 1–63.
9. Hynninen, P. H. Chemistry of Chlorophylls: Modifications. In *Chlorophylls*; Scheer, H., Ed.; CRC: Boca Raton, FL, 1991; pp 145–209.
10. Willstätter, R.; Stoll, A. *Untersuchungen über Chlorophyll*; Springer: Berlin, 1913.
11. Hyvärinen, K.; Hynninen, P. H. *Res. Adv. Org. Bioorg. Chem.* **2001**, *1*, 1–19.
12. Hyvärinen, K. Ph.D. Thesis, University of Helsinki, 2000.
13. Hynninen, P. H.; Assandri, S. *Acta Chem. Scand.* **1973**, *27*, 1478–1486.
14. Hyvärinen, K.; Helaja, J.; Hynninen, P. H. *Tetrahedron Lett.* **1998**, *39*, 9813–9814.
15. Hyvärinen, K.; Hynninen, P. H. *J. Chromatogr. A* **1999**, *837*, 107–116.
16. Hynninen, P. H.; Hyvärinen, K. *J. Org. Chem.* **2002**, *67*, 4055–4061.
17. Hynninen, P. H.; Kavakka, J. S.; Mesilaakso, M. *Tetrahedron Lett.* **2005**, *46*, 1145–1147.
18. Davis, F. A.; Chen, B. *Chem. Rev.* **1992**, *92*, 919–934.
19. Davis, F. A.; Vishwakarma, L. C.; Billmers, J. M.; Finn, J. *J. Org. Chem.* **1984**, *49*, 3241–3243.
20. Ma, L.; Dolphin, D. *Tetrahedron: Asymmetry* **1995**, *6*, 313–316.
21. Ma, L.; Dolphin, D. *J. Org. Chem.* **1996**, *61*, 2501–2510.
22. Fischer, H.; Pfeiffer, H. *Ann. Chem.* **1944**, *555*, 94–110.
23. Kuronen, P.; Hyvärinen, K.; Kilpeläinen, I.; Hynninen, P. H. *J. Chromatogr. A* **1993**, *654*, 93–104.
24. Hyvärinen, K.; Helaja, J.; Kuronen, P.; Kilpeläinen, I.; Hynninen, P. H. *Magn. Reson. Chem.* **1995**, *33*, 646–656.
25. Scheer, H.; Katz, J. J. Nuclear Magnetic Resonance Spectroscopy of Porphyrins and Metalloporphyrins. In *Porphyrins and Metalloporphyrins*; Smith, K. M., Ed.; Elsevier: Amsterdam, 1975; pp 399–523.
26. Katz, J. J.; Brown, C. E. *Bull. Magn. Reson.* **1983**, *5*, 3–49.
27. Abraham, R. J.; Rowan, A. E. Nuclear Magnetic Resonance Spectroscopy of Chlorophyll. In *Chlorophylls*; Scheer, H. Ed.; CRC: Boca Raton, FL, 1991; pp 797–834.
28. Fischer, H.; Stern, A. *Die Chemie des Pyrrols, Vol. 2*; Akademische Verlagsgesellschaft: Leipzig, 1940; Part 2; (Reprinted by Johnson Reprint Corporation: New York, 1968).
29. International Union of Pure and Applied Chemistry (IUPAC) and International Union of Biochemistry (IUB). In *Nomenclature of Tetrapyrroles*; Moss, G. P., Ed.; *Pure Appl. Chem.* **1987**, *59*, 779–832.
30. Holt, A. S. *Can. J. Biochem. Physiol.* **1958**, *36*, 439–456.
31. Hynninen, P. H.; Ellfolk, N. *Acta Chem. Scand.* **1973**, *27*, 1463–1477.

32. Hynninen, P. H. *J. Chromatogr.* **1979**, *175*, 75–88.
33. Hynninen, P. H.; Wasielewski, M. R.; Katz, J. J. *Acta Chem. Scand. B* **1979**, *33*, 637–648.
34. Fales, H. M.; Jaouni, T. M.; Babashak, J. F. *Anal. Chem.* **1973**, *45*, 2302–2303.
35. Kaljurand, I.; Rodima, T.; Pihl, A.; Mäemets, V.; Leito, I.; Koppel, I. A.; Mishima, M. *J. Org. Chem.* **2003**, *68*, 9988–9993.
36. Rodima, T.; Kaljurand, I.; Pihl, A.; Mäemets, M.; Leito, I.; Koppel, I. A. *J. Org. Chem.* **2002**, *67*, 1873–1881.
37. Kaljurand, I.; Rodima, T.; Leito, I.; Koppel, I. A.; Schewesinger, R. *J. Org. Chem.* **2000**, *65*, 6202–6208.
38. Leffek, K.; Przuszynski, P.; Thanapaalasingham, K. *Can. J. Org. Chem.* **1989**, *67*, 590–595.
39. March, J. *Advanced Organic Chemistry. Reactions, Mechanisms, and Structure*, 4th ed.; Wiley: New York, 1992.
40. Hynninen, P. H.; Lötjönen, S. *Org. Magn. Reson.* **1985**, *23*, 605–615.
41. Hynninen, P. H. *Acta Chem. Scand., Ser. B* **1977**, *31*, 829–835.
42. Hynninen, P.H. Unpublished work.
43. Hynninen, P. H.; Lötjönen, S. *Synthesis* **1983**, 705–708.
44. Sahlberg, I.; Hynninen, P. H. *J. Chromatogr.* **1984**, *291*, 331–338.
45. Summers, M. F.; Marzilli, L. G.; Bax, A. *J. Am. Chem. Soc.* **1986**, *108*, 4285–4294.
46. Kilpeläinen, I.; Kaltia, S.; Kuronen, P.; Hyvärinen, K.; Hynninen, P. H. *Magn. Reson. Chem.* **1994**, *32*, 29–35.
47. Friebolin, H. *Basic One- and Two-Dimensional NMR Spectroscopy*, 3rd ed.; Wiley-VCH: Weinheim, 1998; pp 287–300.
48. Günther, H. *NMR Spectroscopy. Basic Principles, Concepts, and Applications in Chemistry*, 2nd ed.; Wiley: Chichester, 1995; pp 397–408.